Two-Photon Interference Using Background-Free Quantum Frequency Conversion of Single Photons Emitted by an InAs Quantum Dot

Serkan Ates,[1,2,*] Imad Agha,[1,2] Angelo Gulinatti,[3] Ivan Rech,[3] Matthew T. Rakher,[1] Antonio Badolato,[4] and Kartik Srinivasan[1,†]

[1]*Center for Nanoscale Science and Technology, National Institute of Standards and Technology, Gaithersburg, Maryland 20899, USA*
[2]*Maryland NanoCenter, University of Maryland, College Park, Maryland, USA*
[3]*Politecnico di Milano, Dipartimento di Elettronica e Informazione, Piazza da Vinci 32, 20133 Milano, Italy*
[4]*Department of Physics and Astronomy, University of Rochester, Rochester, New York 14627, USA*

(Received 17 July 2012; published 4 October 2012)

We show that quantum frequency conversion (QFC) can overcome the spectral distinguishability common to inhomogeneously broadened solid-state quantum emitters. QFC is implemented by combining single photons from an InAs/GaAs quantum dot (QD) at 980 nm with a 1550 nm pump laser in a periodically poled lithium niobate (PPLN) waveguide to generate photons at 600 nm with a signal-to-background ratio exceeding 100:1. Photon correlation and two-photon interference measurements confirm that both the single photon character and wave packet interference of individual QD states are preserved during frequency conversion. Finally, we convert two spectrally separate QD transitions to the same wavelength in a single PPLN waveguide and show that the resulting field exhibits nonclassical two-photon interference.

DOI: 10.1103/PhysRevLett.109.147405 PACS numbers: 78.67.Hc, 42.50.Ar, 42.65.Ky

Quantum frequency conversion (QFC) [1] is a potentially crucial resource in interfacing photonic quantum systems operating at disparate frequencies. Such a hybrid quantum system could, for example, combine robust and stable quantum light sources based on solid-state emitters [2] with broadband quantum memories based on dense atomic ensembles [3] to enable entanglement distribution in a long-distance quantum network [4]. QFC has been enabled by the development of high-efficiency frequency conversion techniques [5,6], and been demonstrated in experiments showing that the quantum character of a light field was preserved during the process [7–13]. In particular, recent experiments have focused on QFC of single photon states, with both frequency up-conversion [10,11] and down-conversion [12,13] of triggered [10,13] and heralded [11,12] sources shown. QFC can be particularly valuable for solid-state quantum emitters, as prominent systems like semiconductor quantum dots [2] and nitrogen vacancy centers in diamond [14] exhibit significant inhomogeneous broadening. Thus, although these systems are in principle scalable, applications which require identical quantum light sources need a mechanism to bring spectrally disparate sources into resonance [15–19]. Unlike previous demonstrations, in which techniques such as strain, optical, or electric fields were applied, QFC can fulfill this role [20] without requiring direct modification of the sources themselves.

Here, we demonstrate nearly background-free QFC, which we use to enable experiments examining photon statistics and two-photon interference of single photons from a semiconductor quantum dot. Compared to previous telecommunications (1300 nm) to visible (710 nm) conversion [10], we work with quantum dots (QDs) emitting in the well-studied 900 nm to 1000 nm wavelength range [2], and convert their single photon emission to 600 nm, a wavelength region in which Si single photon avalanche diodes (SPADs) offer a combination of quantum efficiency and timing resolution that is currently unavailable in the 980 nm band [21]. Using a much wider wavelength separation between signal and pump photons improves the signal-to-background level by about 2 orders of magnitude with respect to Ref. [10]. Measurements of photon statistics and two-photon interference before and after conversion indicate no degradation in purity or wave packet overlap of the single photon stream due to the frequency conversion process. Finally, we show that two spectrally separate transitions of a QD can be converted to the same wavelength in a single periodically poled lithium niobate (PPLN) waveguide, and we present initial measurements demonstrating two-photon interference of these frequency-converted photons. This represents a first step toward a resource-efficient approach in which a single nonlinear crystal acts as a QFC interface that generates indistinguishable photons from different solid-state sources [22].

The basic experimental system is depicted in Fig. 1(a) and described in detail in the Supplemental Material [23]. Our single photon source is an InAs QD in a fiber-coupled, GaAs microdisk optical cavity [24] excited by a continuous wave (cw) or pulsed (50 MHz repetition rate, 50 ps pulse width) 780 nm laser diode. Spectrally isolated emission from the QD can be studied in the 980 nm band through photon correlation and two-photon interference (Hong-Ou-Mandel, [25]) measurements, or else sent to the frequency conversion setup. Frequency conversion is done by combining a strong, tunable 1550 nm pump laser with the

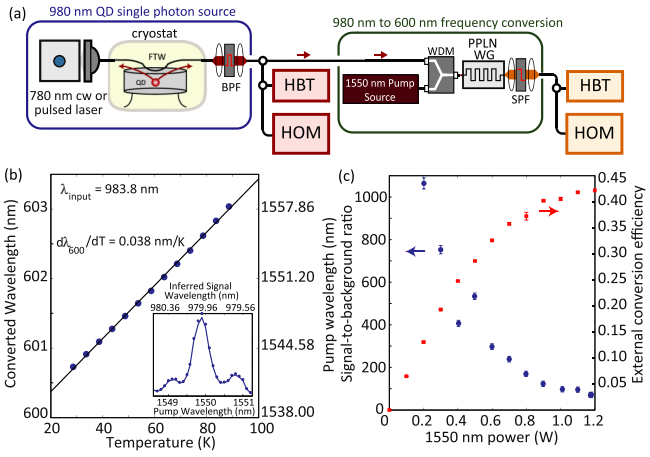

FIG. 1 (color online). (a) Experimental setup used within this work (see the Supplemental Material [23]). HBT = Hanbury-Brown–Twiss setup; HOM = Hong-Ou-Mandel interferometer. (b) Converted 600 nm band wavelength vs PPLN waveguide temperature. The inset shows the quasi-phase-matching response of the PPLN waveguide. (c) Signal-to-background ratio (left y axis, blue points) and external conversion efficiency (right y axis, red points) as a function of 1550 nm pump power. The external conversion efficiency includes all losses in the system.

980 nm QD signal and coupling them into a PPLN waveguide. The 600 nm converted signal is spectrally isolated from frequency-doubled pump light through prisms and short-pass filters, and sent into either a second photon correlation or Hong-Ou-Mandel apparatus, to study the photon statistics and two-photon interference after frequency conversion.

We characterize the frequency conversion setup [23] using an attenuated ($\approx$ 30 fW) 980 nm band laser. First, we measure the quasi-phase-matching bandwidth of the PPLN waveguide, and find that it follows the expected sinc^2 response [5] with an inferred bandwidth in the 980 nm band of $\approx$ 0.20 nm [inset of Fig. 1(b)]. Next, we study how the frequency-converted wavelength changes with PPLN waveguide temperature, which influences phase-matching through thermo-optic and thermal expansion contributions. The resulting plot in Fig. 1(b) indicates that the output wavelength can be tuned by $\approx$ 2 nm. We have also found that signals between 970 nm and >995 nm can be converted (>35% external conversion efficiency) by appropriately adjusting the 1550 nm wavelength and PPLN waveguide temperature. This covers the s-shell emission range of the QD ensemble, and means that QDs emitting at different wavelengths (unavoidable due to size, shape, or composition dispersion during growth) can be converted to the same wavelength.

Ideally, QFC should avoid generating noise photons that are spectrally unresolvable from the frequency-converted quantum state. Sum- and difference-frequency generation in $\chi^{(2)}$ materials are background-free in principle [1], meaning that signal photons are directly converted to idler photons without amplifying vacuum fluctuations. However, other processes, such as frequency conversion of broadband Raman-scattered pump photons, may still be a source of noise, as observed in experiments using PPLN waveguides [26]. To quantify this, the signal-to-background ratio of the converted signal is measured, and reveals the fraction of converted photons originating from the signal rather than noise processes. In previous work [10], the signal-to-background was limited to 7:1, and though use of a pulsed pump removed temporally distinguishable background noise [27], it did not improve the signal-to-background level. While better spectral filtering provides improvement (> 10:1 signal-to-background was reported recently [13]), it is perhaps more desirable to suppress the noise source, for example, by increasing the separation between the signal and red-detuned pump [26,28,29]. Here, our pump-signal separation is nearly 600 nm, suggesting potentially significant improvement.

To test this, we measure [Fig. 1(c)] the signal-to-background level by spectrally isolating the 600 nm conversion band (Supplemental Material [23]) and comparing the detected counts on the SPAD with and without the presence of the 980 nm band signal (the SPAD dark count rate of $\approx$ 50 s^{-1} is subtracted to give a detector-independent metric). We also plot the external conversion efficiency, which includes all PPLN input-output coupling, free-space transmission, and spectral filtering losses (detector quantum efficiency is not included). The signal-to-background level remains above 100 for all but the highest 1550 nm pump powers, where the conversion efficiency has begun to roll off. For the experiments that follow, we operate with a 35% to 40% external conversion efficiency and a signal-to-background level >100. As the PPLN in-coupling efficiency is $\approx$ 60%, and the transmission through all optics after the PPLN waveguide is $\approx$ 80%, the internal conversion efficiency in the PPLN waveguide is >70%.

We now present measurements combining frequency conversion with QD-based single photon sources. We study three devices, $M1$, $M2$, and $M3$, under pulsed and cw excitation conditions. Pulsed measurements are a convenient way to judge the temporal distribution of noise photons produced in the conversion process. Figure 2(a) shows a low-temperature (T = 10 K) microphotoluminescence (μ-PL) spectrum of device $M1$ under 780 nm pulsed excitation. A bright single QD exciton line at 977.04 nm is visible next to a cavity mode at 976.65 nm. The QD emission line was spectrally filtered by a volume Bragg grating whose output was coupled to a single mode fiber [Fig. 2(b) shows the filtered QD emission]. Before performing frequency conversion, this filtered emission was directed to a Hanbury-Brown–Twiss (HBT) setup for photon correlation measurements, the results of which are shown in Fig. 2(c). A strong suppression of the peak at zero time delay to a value of $g^{(2)}(0) = 0.23 \pm 0.04 < 0.5$ is observed. Next, the filtered photoluminescence (PL) was

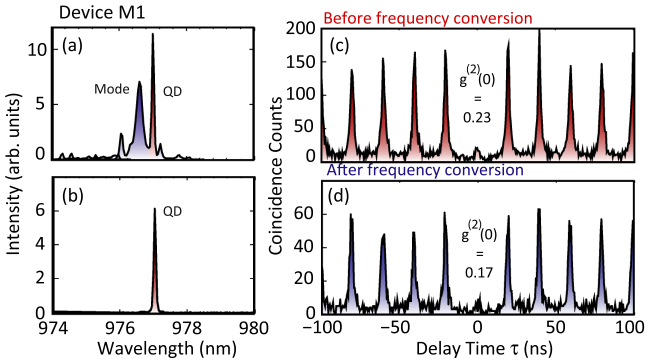

FIG. 2 (color online). (a) Low-temperature μ-PL spectrum of device M1. Bright QD emission and cavity mode emission are visible around 977 nm. (b) Spectrum of QD emission filtered by a volume Bragg grating. (c),(d) Second-order autocorrelation function measurements performed on the QD emission line before and after frequency conversion.

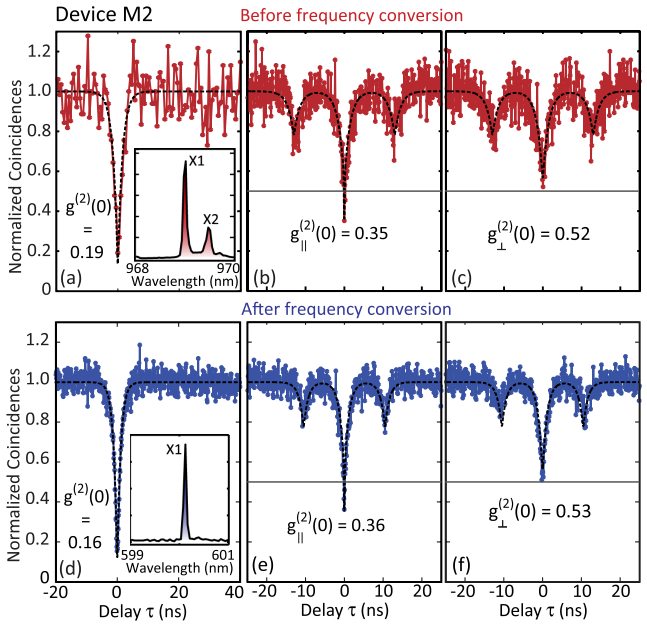

FIG. 3 (color online). (a) Autocorrelation of the $X1$ emission line from device $M2$ under cw excitation (μ-PL spectrum inset). (b),(c) Two-photon interference of the $X1$ line under parallel and orthogonal polarization configurations of the interferometer arms, respectively. (d) Autocorrelation of the $X1$ line after frequency conversion (frequency-converted spectrum inset). (e),(f) Two-photon interference of the frequency-converted $X1$ line under parallel and orthogonal polarization configurations of the interferometer arms, respectively. The dashed lines are fits to the experimental data (Supplemental Material [23]), and the solid line marks $g^{(2)}(0) = 0.5$ level.

sent to the frequency conversion setup, and an autocorrelation measurement was performed on the QD emission after it was converted to 600 nm. As shown in Fig. 2(d), the single-photon nature of the QD emission was preserved during the conversion process, proven by the value of $g^{(2)}(0) = 0.17 \pm 0.03$, and no excess noise from the frequency conversion process was observed. In fact, the additional spectral filtering provided by the quasi-phase-matching process is the likely cause of the reduction in $g^{(2)}(0)$ after frequency conversion, as seen elsewhere [13].

Similar measurements were performed under cw excitation on device $M2$, whose PL spectrum is shown in the inset to Fig. 3(a). Two bright excitonic lines $X1$ and $X2$ are observed on top of a broad cavity mode around 969.5 nm. Figures 3(a) and 3(d) show autocorrelation measurements performed on the filtered $X1$ line before and after frequency conversion to 600 nm, respectively [see inset of Fig. 3(d) for the PL spectrum of the converted signal]. Antibunching dips in Figs. 3(a) and 3(d) [$g^{(2)}_{\mathrm{before}}(0) = 0.19 \pm 0.01$ and $g^{(2)}_{\mathrm{after}}(0) = 0.16 \pm 0.02$] again show that the single photon nature of QD emission is conserved through the frequency conversion process.

In many cases, both single photon purity and single photon indistinguishability [30] are important. At the heart of indistinguishability measurements is two-photon interference [25], which we now show is preserved in our frequency conversion process. Two-photon interference under cw excitation was performed using a fiber-based Mach-Zehnder interferometer [23] similar to Refs. [31,32], where one interferometer arm contains a 12.5 ns delay and a polarization rotator. Rotating the polarization of photons from this arm that are incident on the second beam splitter of the Mach-Zehnder reveals the effect of interference on the photon correlations. In the orthogonal polarization configuration, the interferometer arms are distinguishable and $g_{\perp}^{(2)}(0) = 0.5$ for a pure single photon source. On the other hand, in the parallel polarization configuration, one expects interference between the photons within their coherence time, leading to $g_{\parallel}^{(2)}(0) = 0$. Figures 3(b) and 3(c) show the results of experiments on the $X1$ emission before frequency conversion. The antibunching values are $g_{\parallel}^{(2)}(0) = 0.35 \pm 0.03$ and $g_{\perp}^{(2)}(0) = 0.52 \pm 0.04$, yielding the visibility of two-photon interference as $V = [g_{\perp}^{(2)}(0) - g_{\parallel}^{(2)}(0)]/g_{\perp}^{(2)}(0) = 0.33 \pm 0.08$. The deviation from the ideal value of $V = 1$ stems from the nonzero value of $g^{(2)}(0)$ [Fig. 3(a)] and the time resolution of the photon correlation setup that is on the order of the coherence time (≈ 100 ps) of the QD emission [32]. The same experiments were performed on the $X1$ emission line after frequency conversion, and Figs. 3(e) and 3(f) show the results for parallel and orthogonal polarization configurations, respectively [$g_{\parallel}^{(2)}(0) = 0.36 \pm 0.02$, $g_{\perp}^{(2)}(0) = 0.53 \pm 0.04$]. Because of the conservation of the QD coherence time during the frequency conversion process, we observed a similar two-photon interference visibility $V = 0.32 \pm 0.06$ at 600 nm.

As discussed earlier, a wide wavelength range of QD emission within the 980 nm band can be efficiently

converted to 600 nm by controlling the temperature of the PPLN waveguide and the wavelength of the 1550 nm pump laser. This enables the conversion of well-separated emission lines to the same wavelength at 600 nm. To demonstrate this, both bright emission lines $X1$ and $X2$ from device $M2$ [μ-PL spectrum repeated in Fig. 4(a)] are directed to the frequency conversion setup (see the Supplemental Material [23]), together with two 1550 nm cw pump lasers whose wavelengths are optimized for efficient conversion of the two 980 nm band signals (which are separated by ≈ 0.5 nm). Figure 4(c) shows the PL spectrum of the total converted signal at 600 nm, where the converted signals of the individual $X1$ and $X2$ lines are spectrally overlapped (within the spectrometer's resolution ≈ 40 μeV).

To better understand the nature of the measured emission lines, a cross-correlation measurement was performed before frequency conversion, where the spectrally filtered $X1$ and $X2$ lines were sent to the stop and start channels of the HBT setup, respectively. As shown in Fig. 4(b), a strong asymmetric antibunching dip is observed with $g^{(2)}(0) = 0.26 \pm 0.02$. The antibunching shows that both emission lines originate from the same QD, while the asymmetry is related to the radiative dynamics within the QD. The faster recovery time for $\tau > 0$ can be explained if $X1$ and $X2$ arise from neutral and charged excitonic emission, respectively [33]. This effect arises because emission of the charged exciton $X2$ leaves the QD with a single charge, so that subsequent emission in the neutral exciton state $X1$ requires capture of only a single (opposite) charge. This yields a much faster recovery time than that needed to obtain three charges in the QD, which sets the recovery time for $\tau < 0$.

Next, autocorrelation was performed on the total converted signal at 600 nm, the result of which is shown in Fig. 4(d). As expected, a strong antibunching dip with $g^{(2)}(0) = 0.24 \pm 0.02$ is observed. In contrast to the cross-correlation measurement before conversion, the antibunching dip now has a symmetric shape. This arises from the fact that both QD states were converted within a single PPLN waveguide, so that in the subsequent HBT measurement, the start and stop channels are fed by the same signal at 600 nm, which was composed of both $X1$ and $X2$ emission lines. This mixing of the signals going into the start and stop channels removes the asymmetry observed in the cross-correlation measurement before frequency conversion [Fig. 4(b)].

Finally, we consider two-photon interference from two spectrally distinct QD transitions, as a preliminary step toward using QFC to generate indistinguishable photons from different QDs, which has recently been shown through direct tuning of one of the QD transitions [15,16]. We work with device $M3$, whose spectrum is shown in Fig. 5(a), and which was chosen because the two excitonic states $X1$ and $X2$ have relatively similar intensities. Cross-correlation measurements [23] similar to those described above were performed to confirm that both states come from the same QD. After this, the two states were converted to the same 600 nm wavelength as above, and the combined frequency-converted signal was sent into a Mach-Zehnder interferometer similar to that used earlier. Data from the parallel polarization configuration are shown in Figs. 5(b) and 5(c), where the effect of interference on the photon correlations is seen in the narrow dip at zero time delay, which reaches a value of $g_{\parallel}^{(2)}(0) = 0.13 \pm 0.04$. In comparison, the minimum

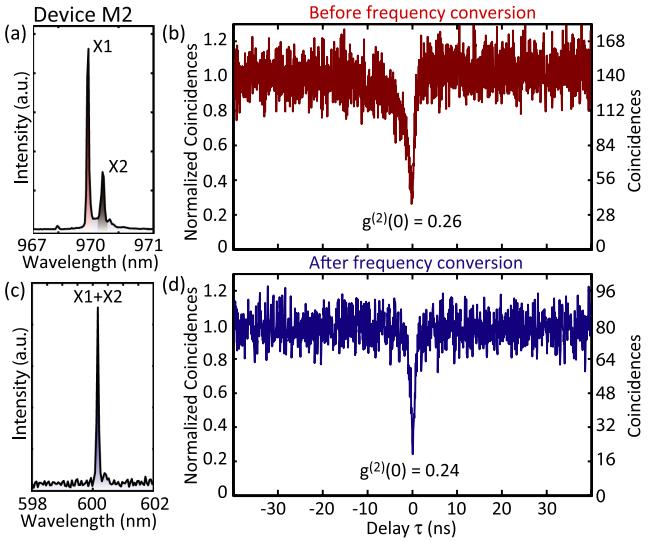

FIG. 4 (color online). (a) μ-PL spectrum of device $M2$ under above-band excitation. (b) Cross-correlation measurement performed on $X1$ and $X2$ emission lines. (c) PL spectrum after both lines are converted to the same wavelength at 600 nm. (d) Autocorrelation measurement of the combined frequency-converted signal of $X1$ and $X2$.

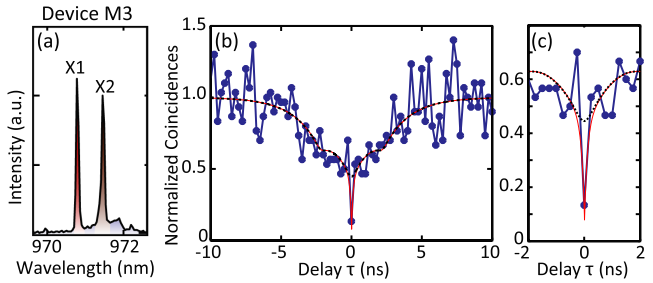

FIG. 5 (color online). (a) μ-PL spectrum of device $M3$ under above-band excitation. Two bright excitonic emission lines (named $X1$ and $X2$) are observed with nearly equal intensity. (b) Two-photon interference of the combined $X1$ and $X2$ signal after both lines are frequency-converted to the same wavelength at 600 nm and measured in the parallel polarization configuration. (c) Zoom-in near the central dip of part (b). The solid red line is a fit to the data, while the black dashed line corresponds to the orthogonal polarization configuration. $g_{\parallel}^{(2)}(0) < g_{\perp}^{(2)}(0)$ is due to the two-photon interference effect.

calculated value (assuming a pure single photon source and infinite timing resolution) for the orthogonal (noninterferring) polarization configuration in our setup (see the Supplemental Material [23]) is $g_{\perp}^{(2)}(0) = 0.36$. This is smaller than the typical value of 0.5 [32] due to the delay $\Delta\tau = 2.2$ ns between the interferometer arms, which is comparable to the average radiative lifetime $T_1 = 1.7$ ns of the two states. Taking into account the nonzero value $g^{(2)}(0) = 0.10$ and the finite timing resolution of the setup, $g_{\perp}^{(2)}(0) = 0.45 \pm 0.04$ is estimated [23], far exceeding the measured value $g_{\parallel}^{(2)}(0) = 0.13 \pm 0.04$, and indicating the significant effect of two-photon interference from the two frequency-converted QD states.

In summary, we have demonstrated background-free quantum frequency conversion of single photons emitted from a quantum dot. Photons at 980 nm are converted to 600 nm with a signal-to-background larger than 100 and external conversion efficiency of 40%. We confirm that single photon purity and wave packet interference are preserved during frequency conversion, and we demonstrate that spectrally distinct QD emission lines can be converted to the same wavelength in the PPLN waveguide. The ability to use a single frequency conversion unit to erase spectral distinguishability in solid-state quantum emitters can be valuable in the development of scalable, chip-based photonic quantum information devices.

We thank Edward Flagg for information on volume Bragg gratings and Lijun Ma and Xiao Tang for discussions about PPLN waveguides. S. A. and I. A. acknowledge support under the Cooperative Research Agreement between the University of Maryland and NIST-CNST 70NANB10H193.

*serkan.ates@nist.gov
†kartik.srinivasan@nist.gov

[1] P. Kumar, Opt. Lett. **15**, 1476 (1990).
[2] A. J. Shields, Nature Photon. **1**, 215 (2007).
[3] K. F. Reim, J. Nunn, V. O. Lorenz, B. J. Sussman, K. C. Lee, N. K. Langford, D. Jaksch, and I. A. Walmsley, Nature Photon. **4**, 218 (2010).
[4] N. Sangouard, C. Simon, J. Minář, H. Zbinden, H. de Riedmatten, and N. Gisin, Phys. Rev. A **76**, 050301 (2007).
[5] M. M. Fejer, G. A. Magel, D. H. Jundt, and R. L. Byer, IEEE J. Quantum Electron. **28**, 2631 (1992).
[6] A. H. Gnauck, R. Jopson, C. McKinstrie, J. Centanni, and S. Radic, Opt. Express **14**, 8989 (2006).
[7] J. M. Huang and P. Kumar, Phys. Rev. Lett. **68**, 2153 (1992).
[8] G. Giorgi, P. Mataloni, and F. De Martini, Phys. Rev. Lett. **90**, 027902 (2003).
[9] S. Tanzilli, W. Tittel, M. Halder, O. Alibart, P. Baldi, N. Gisin, and H. Zbinden, Nature (London) **437**, 116 (2005).
[10] M. T. Rakher, L. Ma, O. Slattery, X. Tang, and K. Srinivasan, Nature Photon. **4**, 786 (2010).
[11] H. J. McGuinness, M. G. Raymer, C. J. McKinstrie, and S. Radic, Phys. Rev. Lett. **105**, 093604 (2010).
[12] R. Ikuta, Y. Kusaka, T. Kitano, H. Kato, T. Yamamoto, M. Koashi, and N. Imoto, Nature Commun. **2**, 537 (2011).
[13] S. Zaske, A. Lenhard, C. A. Kessler, J. Kettler, C. Hepp, C. Arend, R. Albrecht,W.-M. Schulz, M. Jetter, P. Michler, and C. Becher, preceding Letter, Phys. Rev. Lett. **109**, 147404 (2012)..
[14] C. Kurtsiefer, S. Mayer, P. Zarda, and H. Weinfurter, Phys. Rev. Lett. **85**, 290 (2000).
[15] E. B. Flagg, A. Muller, S. V. Polyakov, A. Ling, A. Migdall, and G. S. Solomon, Phys. Rev. Lett. **104**, 137401 (2010).
[16] R. B. Patel, A. J. Bennett, I. Farrer, C. A. Nicoll, D. A. Ritchie, and A. J. Shields, Nature Photon. **4**, 632 (2010).
[17] R. Lettow, Y. L. A. Rezus, A. Renn, G. Zumofen, E. Ikonen, S. Götzinger, and V. Sandoghdar, Phys. Rev. Lett. **104**, 123605 (2010).
[18] H. Bernien, L. Childress, L. Robledo, M. Markham, D. Twitchen, and R. Hanson, Phys. Rev. Lett. **108**, 043604 (2012).
[19] A. Sipahigil, M. L. Goldman, E. Togan, Y. Chu, M. Markham, D. J. Twitchen, A. S. Zibrov, A. Kubanek, and M. D. Lukin, Phys. Rev. Lett. **108**, 143601 (2012).
[20] H. Takesue, Phys. Rev. Lett. **101**, 173901 (2008).
[21] M. Ghioni, A. Gulinatti, I. Rech, F. Zappa, and S. Cova, IEEE J. Sel. Top. Quantum Electron. **13**, 852 (2007).
[22] K. Sanaka, A. Pawlis, T. D. Ladd, K. Lischka, and Y. Yamamoto, Phys. Rev. Lett. **103**, 053601 (2009).
[23] See Supplemental Material http://link.aps.org/supplemental/10.1103/PhysRevLett.109.147405 for details regarding experimental setups, measurements, and data analysis.
[24] K. Srinivasan and O. Painter, Nature (London) **450**, 862 (2007).
[25] C. K. Hong, Z. Y. Ou, and L. Mandel, Phys. Rev. Lett. **59**, 2044 (1987).
[26] C. Langrock, E. Diamanti, R. Roussev, Y. Yamamoto, M. Fejer, and H. Takesue, Opt. Lett. **30**, 1725 (2005).
[27] M. T. Rakher, L. Ma, M. Davanço, O. Slattery, X. Tang, and K. Srinivasan, Phys. Rev. Lett. **107**, 083602 (2011).
[28] J. S. Pelc, L. Ma, C. R. Phillips, Q. Zhang, C. Langrock, O. Slattery, X. Tang, and M. M. Fejer, Opt. Express **19**, 21445 (2011).
[29] H. Dong, H. Pan, Y. Li, E. Wu, and H. Zeng, Appl. Phys. Lett. **93**, 071101 (2008).
[30] C. Santori, D. Fattal, J. Vuckovic, G. Solomon, and Y. Yamamoto, Nature (London) **419**, 594 (2002).
[31] A. Kiraz, M. Ehrl, T. Hellerer, O. E. Müstecaplıoğlu, C. Bräuchle, and A. Zumbusch, Phys. Rev. Lett. **94**, 223602 (2005).
[32] R. B. Patel, A. J. Bennett, K. Cooper, P. Atkinson, C. A. Nicoll, D. A. Ritchie, and A. J. Shields, Phys. Rev. Lett. **100**, 207405 (2008).
[33] A. Kiraz, S. Falth, C. Becher, B. Gayral, W. V. Schoenfeld, P. M. Petroff, L. Zhang, E. Hu, and A. Imamoglu, Phys. Rev. B **65**, 161303 (2002).